DOI: 10.1002/asia.200800300

Preparation of Core-shell Magnetic Molecularly Imprinted Polymer Nanoparticles for Recognition of Bovine Hemoglobin

Lin Li,[a] Xiwen He,[a] Langxing Chen,*[a] and Yukui Zhang*[a, b]

Abstract: In this work, the core-shell bovine hemoglobin (BHb) imprinted magnetic nanoparticles (MNPs) with a mean diameter of 210 nm were synthesized for the first time. In this protocol, the initial step involved co-precipitation of Fe^{2+} and Fe^{3+} in an ammonia solution. Silica was then coated on the Fe_3O_4 nanoparticles using a sol-gel method to obtain silica shell magnetic nanoparticles. Subsequently, 3-aminophenylboronic acid (APBA), which is the functional and cross-linking monomer, and poly(APBA) thin films were coated onto the silica-modified Fe_3O_4 surface through oxidation with ammonium persulfate in an aqueous solution in the presence or absence of protein. The morphology, adsorption, and recognition properties of the magnetic molecularly imprinted nanomaterial were investigated by transmission electron microscopy (TEM), X-ray diffraction (XRD), thermogravimetric analysis (TGA), and vibrating sample magnetometer (VSM). Rebinding experiments were carried out to establish the equilibrium time and to determine the specific binding capacity and selective recognition. The protein adsorption results showed that poly(APBA) MIPs-coated magnetic nanoparticles have high adsorption capacity for template protein BHb and comparatively low non-specific adsorption. The imprinted magnetic nanoparticles could easily reach the adsorption equilibrium and magnetic separation under an external magnetic field, thus avoiding problems related to the bulk polymer. We believe that the imprinted polymer-coated magnetic nanoparticles can be one of the most promising candidates for various applications, which include chemical and biochemical separation, cell sorting, recognition elements in biosensors, and drug delivery.

Keywords: adsorption · imprinting · magnetic properties · nanoparticles · thin films

Introduction

Magnetic nanoparticles (MNPs), of which superparamagnetic iron oxide (SPIO) is a representative example, have attracted increasing attention in the fields of biomedical and biotechnological applications, which includes targeted drug delivery, magnetic resonance imaging (MRI) contrast enhancement, and separation and purification of proteins and cells,[1,2] because of their small size and high surface-to-volume ratio. In comparison with conventional micrometer-size resins or beads, MNPs have many superior characteristics for bioseparation applications, such as good dispersability, fast and effective binding to biomolecules, and reversible and controllable flocculation.[3] The magnetic separation process can be performed directly in crude samples containing suspended solid particles or other biological particulates in a rapid and easy way. Moreover, the power and efficiency of magnetic separation is especially useful for large-scale operations.[4] For many of these applications, surface modification of MNPs is the key challenge. In general, surface modification can be accomplished by physical/chemical adsorption or surface coating with specific ligands depending on the specific application to the biomedical and biotechnological fields. When modified with a specific functional polymer, for example the molecularly imprinted polymers (MIPs), the functional materials are able to recognize and in some cases respond to biological and chemical agents of interest. These MIP-coated MNPs would be able to separate and concentrate chemicals more conveniently with the help of an external magnetic field.

The molecular imprinting technique is an attractive method for the generation of tailored materials that have

[a] Dr. L. Li, Prof. X. He, Prof. L. Chen, Prof. Y. Zhang
Department of Chemistry
Nankai University
Tianjin 300071 (P.R. China)
Fax: (+86) 22-23502458
E-mail: lxchen@nankai.edu.cn

[b] Prof. Y. Zhang
Dalian Institute of Chemical Physics
Chinese Academy of Sciences
Dalian 116011 (P.R. China)

the ability to recognize and in some cases respond to biological and chemical agents of interest.[5–7] The technique involves polymerization of functional monomers and a cross-linker around a template. The removal of the template leaves behind the imprinted specific recognition sites with the function, size, and shape complementary to the template. MIPs have been used in a variety of applications, as separation media,[8,9] for mimicking antibodies,[10] chemical and biochemical sensing,[11] and drug delivery.[12] In contrast to its biological counterparts, enzymes and antibodies, MIPs display significant advantages such as high mechanical/chemical stability, low cost, ease of preparation, and predictable specific recognition. Although MIPs have been successfully developed against a wide range of small molecules, the imprinting of macromolecules like proteins has proven to be more problematic. Some disadvantages, such as entrapment of the macromolecular template in the polymer matrix, poor mass transfer, low integrity of the polymer structure, and the production of heterogeneous binding sites, arising from the geometric and chemical complexity of proteins, have also been observed.[13,14] To resolve these problems, surface imprinting has been proposed as a viable strategy for protein imprinting. An ultrathin polymer coating on a solid support substrate using the surface imprinting approach can improve the mass transfer and reduce permanent entrapment of the protein template, but these methods also reduce the number of imprinted sites.[15–23]

3-aminophenylboronic acid (APBA) is an attractive functional monomer for protein imprinting being water-soluble and thus providing a mild aqueous environment during polymerization. Additionally, it also provides a variety of favorable and reversible interactions with the amino acids on the protein. Many biotechnological applications, like bioseparation and biosensing, would employ MIPs as a surface coating on a solid material, to potentially overcome mass transfer limitations and non-quantitative recovery of the template molecule. The ultrathin poly(APBA) films have been fabricated as surface coatings on solid support substrates such as a polystyrene microwell plate and microsphere, a glass slide, and the gold surface of a quartz crystal microbalance (QCM) electrode.[15,18–21]

Therefore, combining magnetic separation and molecular imprinting would ideally provide a powerful analytical tool having the characteristics of simplicity, flexibility, and selectivity. By incorporating magnetic iron oxide, superparamagnetic composite MIP beads with an average diameter of 13 μm were prepared using suspension polymerization in perfluorocarbon for the first time.[24] Recently, protein surface-imprinted sub-micrometer particles with magnetic susceptibility using mini-emulsion polymerization has been reported.[23] In this work, we have reported the synthesis of core-shell bovine hemoglobin imprinted magnetic nanoparticles. Compared to traditional MIPs, the MIPs prepared on the surface of iron oxide would be ideal as a multifunctional nanomaterial towards bioseparation. Thus, molecular imprinted magnetic nanoparticles, having a small dimension with a high surface-to-volume ratio, are expected to improve the removal of template molecules. The binding capacity and fast binding kinetics, and the superparamagnetic iron oxide core enables the MIP particles to replace the centrifugation step with magnetic separation, and facilitates the application of magnetic MIPs in immunoassay and magnetically stabilized fluidized bed separation. In this article, we present a technique for the preparation of core-shell protein MIP-coated magnetic nanoparticles (Figure 1). Nanosized Fe_3O_4 MNPs were prepared using a coprecipitation method, and then the silica shell was deposited. Subsequently, poly(APBA) thin films were coated onto the silica-modified Fe_3O_4 surface through polymerization, where APBA is the functional and cross-linking monomer. Finally, the template protein was removed by repetitive washing with copious amounts of deionized water and washing buffer. The morphology, adsorption, and recognition properties of these magnetic molecularly imprinted nanomaterials have been investigated.

Abstract in Chinese:

本工作首次合成了平均粒径210nm核壳结构的牛血红蛋白印迹磁性纳米粒子。首先在氨水溶液中通过Fe^{2+}和Fe^{3+}共沉淀合成四氧化三铁纳米粒子。采用溶胶凝胶法制备硅包覆在Fe_3O_4表面的硅壳磁性纳米粒子；然后使用间氨基苯硼酸作为功能单体和交联剂，分别在水溶液中有模板蛋白质和没有模板蛋白质存在的情况下，通过过硫酸铵氧化在硅修饰的Fe_3O_4表面形成聚间氨基苯硼酸薄层。通过透射电子显微镜、X射线衍射、热重分析、振动样品磁强计研究了分子印迹磁性纳米材料的形态、吸附、识别性能。蛋白质的吸附结果表明包覆聚间氨基苯硼酸分子印迹聚合物的磁性纳米粒子对模板蛋白质BHb具有高吸附能力和相对低的非特异吸附。这种印迹磁性纳米粒子容易达到吸附平衡，并且在外加磁场下容易磁性分离。因此，表面为印迹聚合物修饰的磁性纳米粒子在化学和生化分离、细胞筛选、生物传感器、药物传输等领域具有很好的应用前景。

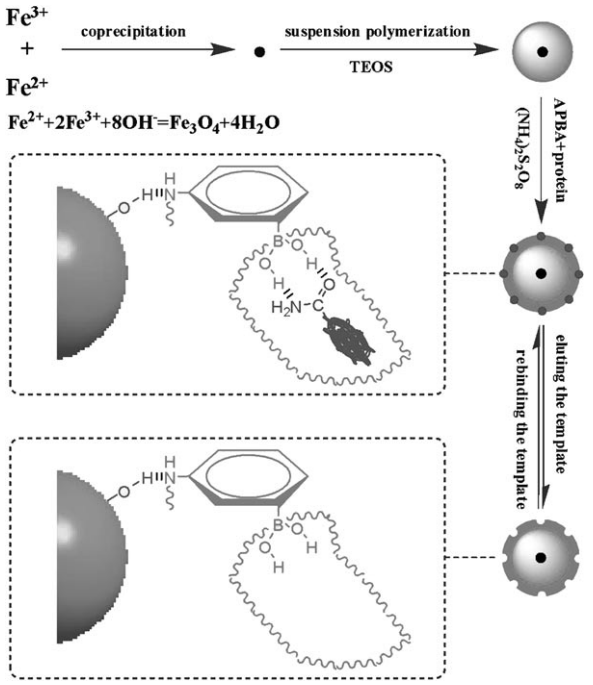

Figure 1. Schematic illustration of the preparation of magnetic molecularly imprinted nanoparticles.

Results and Discussion

Synthesis of Superparamagnetic MIP-coated Nanoparticles

The synthesis of the MIP-coated MNPs through a multistep procedure is illustrated in Figure 1, which involves synthesis of the Fe_3O_4 MNPs, silica-shell deposition, coating poly(APBA) film onto the silica surface, and final extraction of the template protein and generation of the recognition site. First, superparamagnetic Fe_3O_4 nanoparticles were prepared by the coprecipitation method.[25] It is known that the critical particle size of superparamagnetism of magnetic particles is 25 nm. Therefore, the prepared magnetic Fe_3O_4 nanoparticles have to be less than 25 nm in order to ensure that they possess superparamagnetic properties. Secondly, because of the anisotropic dipolar attraction, unmodified MNPs tend to aggregate into large clusters and thus lose the specific properties of a single-domain. The formation of a silica coating on the surfaces of iron oxide nanoparticles could provide a good biocompatible, non-toxic coating as well as a hydrophilic surface, and thus prevent aggregation in liquid. The silica shell helps to avoid electrostatic agglomeration because of the low isoelectric point (about 2–3) of silica and therefore the silica-coated nanoparticles display a significant negative surface charge at the pH employed in the experiment. Furthermore, the terminated silanol groups on the silica coating offer many possibilities for surface functionalization through covalent attachment of specific ligands on the surfaces of these MNPs.[26,27] The growth of silica shells on Fe_3O_4 nanoparticles was developed by a sol-gel process using tetraethyl orthosilicate (TEOS).[27] Finally, poly(APBA) thin films were coated onto the silica shells of the magnetic silica nanoparticles by molecular imprinting process. In an aqueous solution, the template protein and the functional monomer APBA form a complex through interactions between the $-B(OH)_2$ group on APBA and the amino acids on the template protein.[15] Poly(APBA) polymer can be easily synthesized by the chemical oxidation of APBA and can be grafted tightly to the surface of polystyrene microplate[19] and microsphere,[18] glass and gold of quartz crystal microbalance electrodes.[20,21] The silica shells on Fe_3O_4 nanoparticles have a strong affinity to APBA, therefore the complex is grafted onto the surface of the magnetic silica nanoparticles by the chemical oxidation of APBA. After washing with 0.2 M sodium phosphate buffer (pH 9.0) containing 0.5 M sorbitol until no further template protein could be monitored, the MIP-coated MNPs with imprinted recognition sites on the layer of the MNPs were obtained.

Characterization of the Synthesized Nanoparticles

Representative transmission electron microscopy (TEM) images of magnetite, magnetite@silica and poly(APBA) MIP-coated MNPs are provided in Figure 2. From these images, it is obvious that all of these particles are nano-sized and roughly spherical in shape before and after being encapsulated by silica and APBA. Figure 2a shows the TEM image of the uncoated Fe_3O_4 nanoparticles. This image reveals an homogeneous size distribution with a mean diameter of about 12 nm. Figure 2b shows the TEM image of the magnetite@silica nanoparticles with a mean diameter of 200 nm, clearly showing that the magnetite nanoparticles were fully coated by the silica. This provides the magnetite core with a silica surface, which favors the encapsulation of MNPs by polymers. Figure 2c shows the distinct core-shell structure of the poly(APBA) film-coated silica nanoparticles, with a 10 nm thin layer of APBA on the surface of silica-coated MNPs and complete coverage of the core by APBA. This image suggests that core-shell nanoparticles with more regular morphological features were prepared through a step-by-step coating procedure. This image also reveals that the coating process did not significantly result in the agglomeration and change in size of particles, which can be attributed to the fact that the reaction occurred only on the particle surface. The particle size increases slightly after the coating with APBA, with a mean diameter of about 210 nm, which is slightly larger than that of silica-coated MNPs.

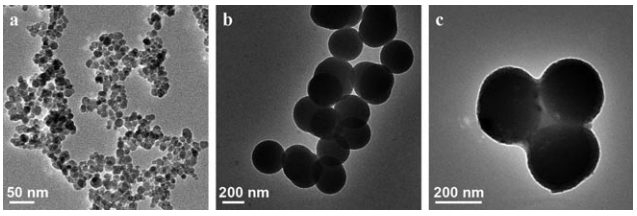

Figure 2. TEM images of a) Fe_3O_4 magnetic nanoparticles, b) silica-coated MNPs and c) poly(APBA) MIP-coated MNPs.

Thermogravimetric analysis (TGA) was performed to further estimate the relative composition of the nano-core and the organic shell. Figure 3 shows a representative set of the weight loss for a) silica-coated MNPs and b) poly(APBA) MIP-coated MNPs. All nanoparticle samples displayed a similar mass-loss profile for the release of physically ad-

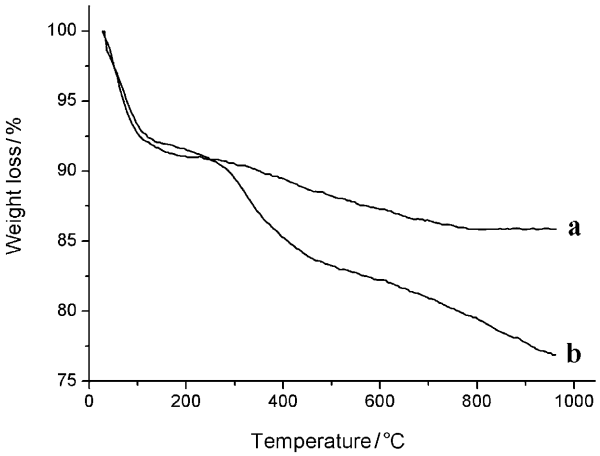

Figure 3. TGA of MNPs a) silica-coated MNPs and b) poly(APBA) MIP-coated MNPs.

sorbed solvent or water and organic capping materials. The amount of solvent or water released corresponds to approximately 8% at T < ~120 °C. For the organic mass-loss at approximately 300 °C < T < ~400 °C, the silica nanoparticles with APBA revealed a slightly high organic mass release of ~7%. The compound completely decomposed at temperatures above 400 °C and the silica coating began to slowly decompose. Both the magnetite content and silica coating content of the nanoparticles were evaluated to be approximately 85%.

From the above-mentioned TGA analysis, the coating of the silica shell on Fe_3O_4 magnetic nanoparticles indeed was quite efficient for the improvement of their stability and activity for further application.

Figure 4 shows the X-ray diffraction (XRD) patterns for the magnetic nanoparticles with and without coating. In the 2θ range of 20–70°, six characteristic peaks for Fe_3O_4 (2θ = 30.1°, 35.5°, 43.1°, 53.4°, 57.0°, and 62.6°) were observed for the three samples, and the peak positions at the corresponding 2θ value were indexed as (220), (311), (400), (422), (511), and (440), respectively, which match well with the database of magnetite in the JCPDS-International Center for Diffraction Data (JCPDS Card: 19-629).

The diffraction peaks are labeled with the indexed Bragg reflections spectra of the Fe_3O_4 structure. The XRD patterns show the presence of the characteristic diffraction peaks of magnetite/maghemite for the synthesized particles, which are highly crystalline materials. The XRD patterns also reveal that the synthesized particles contain Fe_3O_4 with a spinel structure[28] and the binding process did not result in the phase change of Fe_3O_4. XRD analysis cannot discriminate between magnetite (Fe_3O_4) and its oxidation product maghemite (γ-Fe_2O_3) because both diffraction patterns overlap and are nearly identical. Even if we have a mixture of both oxides, because both these oxides are magnetic and the surface states of either phase allow the growth of a silica shell, it is not considered important to determine the relative percentages of these phases in these samples.

The peak positions were unchanged while their widths had increased, which indicates that the crystal structure was substantially unchanged. The intensity of the XRD peaks decreased after coating the particles with silica because of the effect of the amorphous silica shell. The difference in peak width for the three types of

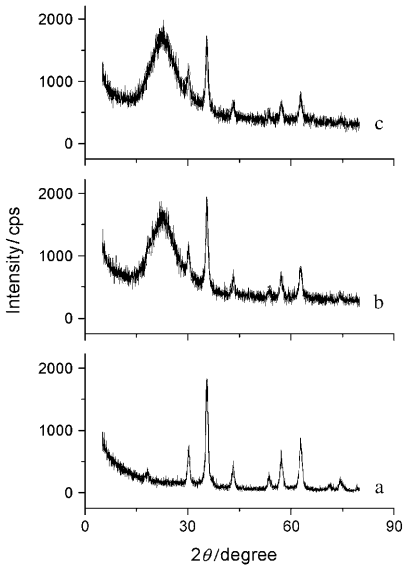

Figure 4. X-ray diffraction patterns of a) Fe_3O_4 magnetic nanoparticles, b) silica-coated MNPs and c) poly(APBA) MIP-coated MNPs.

nanoparticles reflected the differences in their average particle size. As the particle sizes get larger, the XRD peaks display slightly narrower peak widths.

Vibrating sample magnetometry (VSM) was employed to study the magnetic properties of the synthesized MNPs, and the magnetic hysteresis loop of the dried samples at room temperature is illustrated in Figure 5. From the VSM data, the remnant magnetization (M_r), coercivity (H_c), and

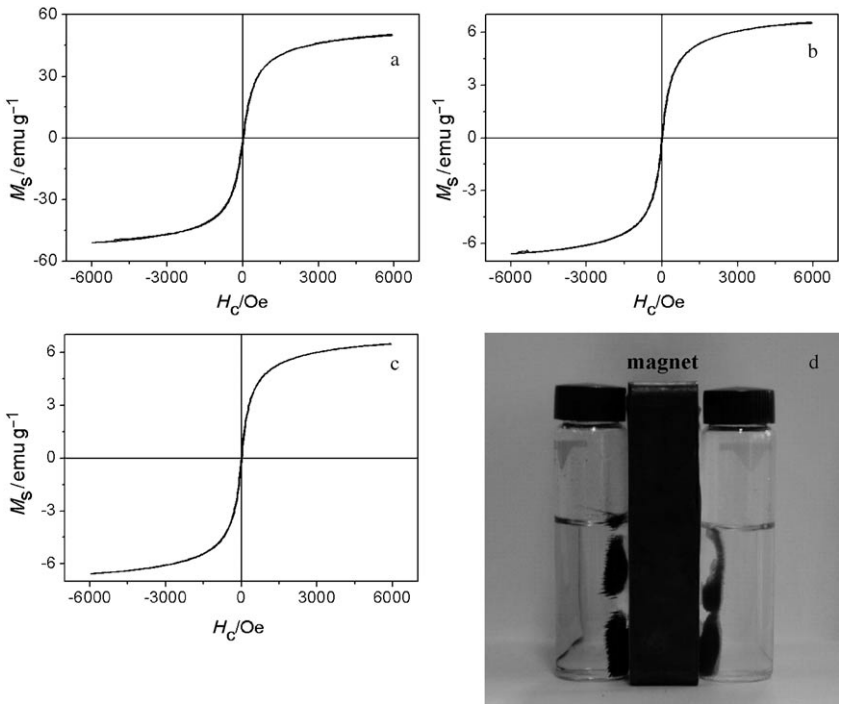

Figure 5. Hysteresis loops of a) Fe_3O_4 nanoparticles, b) silica-coated MNPs and c) poly(APBA) MIP-coated MNPs; d) The separation process of the nanoparticles in distilled water (black MNPs on the left: uncoated Fe_3O_4 nanoparticles; yellow MNPs on the right: silica-coated MNPs).

squareness ($S_r = M_r/M_s$) can be determined. The values of M_r, H_c and S_r are 1.673 emu g^{-1}, 20.26 Oe, and 0.033 for the uncoated magnetic nanoparticles, 0.2988 emu g^{-1}, 17.51 Oe, and 0.045, for silica-coated MNPs and 0.2852 emu g^{-1}, 16.66 Oe, and 0.044, for poly(APBA) MIP-coated MNPs, respectively. The very weak hysteresis confirmed that the uncoated MNPs, silica-coated MNPs and poly(APBA) MIP-coated MNPs have superparamagnetic properties at room temperature, which implies that the sample retains no remnant in the absence of an external magnetic field environment. In the presence of an external magnetic field, black MNPs on the left of the magnet (i.e., uncoated MNPs) and yellow MNPs on the right of the magnet (i.e., silica-coated MNPs) were attracted to the wall of the vial and the dispersed liquid became clear and transparent (Figure 5d). The MNPs' color change from black to yellow could be attributed to the oxidation of a little amount of Fe_3O_4 to γ-Fe_2O_3 during the silanization process. Since both Fe_3O_4 and γ-Fe_2O_3 have similar magnetic properties, the presence of trace amounts of oxide is not important in the present study. The superparamagnetism prevents MNPs from aggregating and enables them to redisperse rapidly when the magnetic field is removed. This can be attributed to the fact that the magnetic core is so small (average particle size is 12 nm) that they may be considered to have a single magnetic domain.

The saturation magnetization of silica-coated MNPs and poly(APBA) MIP-coated MNPs was 6.582 emu g^{-1} and 6.536 emu g^{-1}, respectively, which is lower than that of the uncoated Fe_3O_4 magnetic nanoparticles (50.69 emu g^{-1}). The M_s value for poly(APBA) MIP-coated MNPs was slightly lower than that for the silica-coated MNPs. These results indicate that the modification reaction on the particle surface had a strong impact on the magnetism of the nanospheres, which might quench the magnetic moment. As a result of such high saturation magnetization, which makes them very susceptible to magnetic fields, the nanoparticles could be easily and quickly separated from a suspension. This is very favorable for the magnetic separation of proteins on a large scale.

Adsorption Kinetics

Figure 6a presents the adsorption kinetics of 0.2 mg mL^{-1} BHb solution onto MIP. We can see that the adsorption capacity increased with time and the imprinted nanoparticles had a fast adsorption rate. In the first 80 min, the adsorption increased rapidly; after 80 min the adsorption had almost reached an equilibrium. This time profile indicates an initial rapid increase in the adsorption capacity and then a slower approach to a limiting value. For the imprinted materials of non-thin films, it takes generally 12–24 h to reach adsorption equilibrium.[29] However, the imprinted materials of thin films need only 30–120 min to reach adsorption equilibrium for biomacromolecule templates. Therefore, in our case, BHb molecules reached the surface imprinting cavities of MIP easily and took less time to reach adsorption saturation, which implies that poly(APBA) MIP-coated MNPs has the property of good mass transport and thus overcomes some drawbacks of traditional packing imprinted materials.

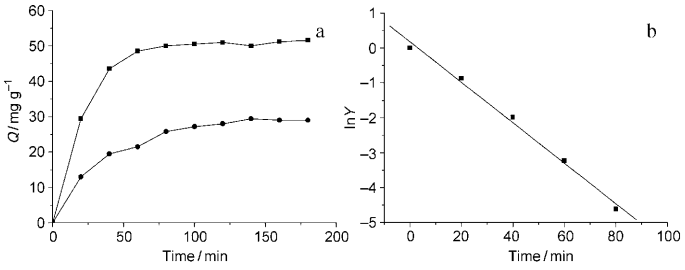

Figure 6. a) Curve of adsorption kinetics (■ MIP, ● NMIP; C_{BHb} = 0.2 mg mL^{-1}; $m_{MIP} = m_{NIP} = 15.0$ mg; pH = 7.2; $T = 25$ °C); b) Plot of ln Y versus t.

This process can be described as an apparent first-order kinetic process:[30]

$$-dC/dt = kC \quad (1)$$

Integration of Eq. (1) gives:

$$C = C_0 \exp(-kt) \quad (2)$$

Here C_0 and C are the original and actual concentrations of the template protein, respectively, and k is the apparent rate constant of protein adsorption. So the amount of adsorption capacity with time would be:

$$Q = Q_e [1 - \exp(-kt)] \quad (3)$$

To use conveniently, one can rearrange Eq. (3) into the following form:

$$\ln Y = -kt,\ Y = (Q_e - Q)/Q_e \quad (4)$$

Here Q_e and Q are the final equilibrium adsorption capacity and the actual adsorption capacity, respectively. According to Eq.4, a plot of ln$Y$ versus t would be a straight line (Figure 6b). The apparent rate constant, which characterizes the rate of protein adsorption, was obtained from the slope of the linear fit and was found to be 5.5×10^{-2}.

Adsorption Isotherm

A general method to study the thermodynamic adsorption properties of MIP is the adsorption isotherms curve. Adsorption experiments were carried out at room temperature. After 80 min incubation, which was sufficient to reach the adsorption equilibrium, the solutions were centrifuged, and their concentrations were measured by a UV/Vis spectrophotometer. Figure 7a shows the adsorption isotherms of BHb solutions on BHb-imprinted nanoparticles. From Figure 7a, we can see that when C_o was below 0.2 mg mL^{-1}, the adsorption capacity increased quickly; however, when C_o was over 0.2 mg mL^{-1}, the adsorption curve became relatively flat. This indicates that the amount (Q_e) of protein ad-

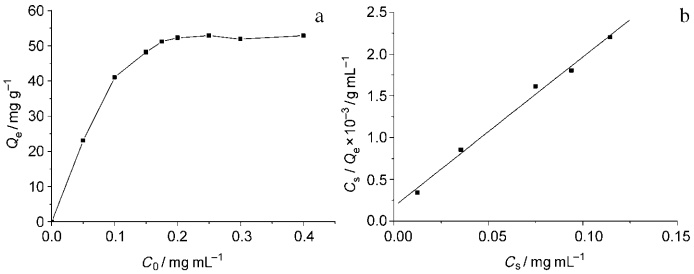

Figure 7. a) Curve of adsorption isotherm (m_{MIP} = 30.0 mg; pH = 7.2; T = 25 °C); b) Curve of C_s/Q_e versus C_s.

sorbed onto MIP or NMIP (non-imprinted polymers) increased as the concentration (C_0) of the protein solutions increased and that the imprinted nanoparticles had specific adsorption within the range of the experimental concentrations (Q_e is the equilibrium adsorption capacity and C_0 is the original protein concentration). The recognition sites on the surface of imprinted nanospheres have better steric matching with the template protein, which allows imprinted thin films to adsorb more template protein molecules.

The shape of the adsorption curve was similar to that of the Langmuir adsorption curve (Figure 7b). According to Langmuir's isotherm equation,

$$C_s/Q_e = C_s/Q_o + 1/(KQ_o) \quad (5)$$

Here, Q_o is the saturated adsorption capacity, C_s is the substrate concentration after adsorption equilibrium, and K is the adsorption constant. The plot of C_s/Q_e versus C_s is linear over the investigated concentration range, which demonstrates that the adsorption isotherm of MIP agrees with the Langmuir adsorption model. From the slope of the linear fit, we can find that Q_o is about 55.87 mg g^{-1}. It is interesting that this kind of nanoparticle has a high adsorption capacity for the template protein, something which is rarely reported in the literature.

Ability to Recognize the Template Protein

To confirm the selective recognition of the MIP, we selected bovine serum albumin (BSA) as the control. BSA is a most representative and appropriate model because the molecular weight and volume of the BSA molecule is similar to that of the BHb molecule. The solutions were filtered, and the protein concentrations were measured after an 80 min incubation at room temperature. To test the selective recognition of MIP, the same experiments were carried out with non-MIP. The imprinting factor (α) of BHb-MIP, defined as the ratio of adsorption quantities of BHb-MIP to that of NMIP ($\alpha = Q_{MIP}/Q_{NMIP}$) was found to be 1.803. The separation factor (β) of BHb-MIP, which is defined as the ratio of adsorption quantity of template (BHb) to that of competitor molecules (BSA) ($\beta = Q_{BHb}/Q_{BSA}$), was found to be 1.966. It is suggested that, in the case of BHb-MIP, its adsorption quantity for BHb is more than that for the competitor protein in the same solution. The experimental results (Figure 8) illuminate that specific recognition sites for BHb are formed during the course of imprinting and thin films of imprinted nanoparticles are able to selectively adsorb template proteins.

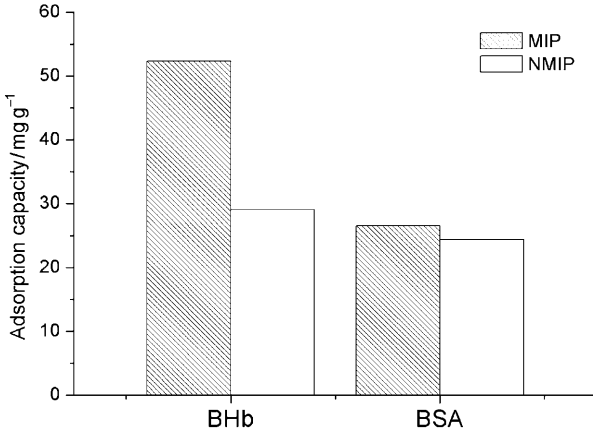

Figure 8. Adsorption selectivity of BHb-MIP and NIP for BHb and BSA, respectively ($C_{BHb} = C_{BSA}$ = 0.2 mg mL^{-1}; $m_{MIP} = m_{NMIP}$ = 15.0 mg; pH 7.2; T = 25 °C; t = 5 h).

Conclusions

We have constructed superparamagnetic molecularly imprinted nanomaterials by coating thin films of functional monomer (APBA) onto the surface of silica-coated MNPs in an aqueous solution with BHb as the template. The method of coating silica nanoparticles with APBA overcomes the drawback of monolith materials of hindering protein molecules from diffusion. The results indicated that the imprinted nanoparticles that possess specific recognition sites on the shells have specific selectivity for the initially imprinted template protein and high stability and can make protein molecules attain diffusion-controlled equilibrium within 80 min. Moreover, this kind of nanoparticle has high adsorption capacity and selective recognition for the template protein. All these results demonstrate that the superparamagnetic molecularly imprinted nano-composite has potential applications in the separation and detection of biomacromolecules so as to enable high abundance of protein to be removed and low abundance of protein to be enriched in proteomics.

Experimental Section

Materials

3-Aminophenylboronic acid monohydrate was obtained from Beijing Element Chem.-Tech. Company (Beijing, China). Ammonium persulphate ($(NH_4)_2S_2O_8$) was obtained from Tianjin North Tianyi Chemical Reagent Factory (Tianjin, China). Bovine serum albumin (BSA, MW 68 kDa, pI = 4.9) was obtained from Beijing Dingguo Bio.-Tech. Company (Beijing, China). BHb (MW 68 kDa, pI = 6.8 ~ 7.2) was obtained from Shanghai

Lanji Chem.-Tech. Company (Shanghai, China). Deionized water was used for all experiments.

All other materials used were of analytical grade and commercially available, including ferric chloride hexahydrate ($FeCl_3 \cdot 6H_2O$), ferrous chloride tetrahydrate ($FeCl_2 \cdot 4H_2O$), ammonium hydroxide (25% w/w), tetraethyl orthosilicate (TEOS) and 2-propanol.

Synthesis

Superparamagnetic magnetite nanoparticles: An aqueous suspension of superparamagnetic magnetite nanoparticles were prepared by the controlled chemical coprecipitation reaction. $FeCl_2 \cdot 4H_2O$ (3.44 g) and $FeCl_3 \cdot 6H_2O$ (9.44 g) were respectively dissolved under a N_2 atmosphere in deaerated deionized water (160 mL) with vigorous mechanical stirring (800 rpm). A nitrogen gas environment was maintained in the vessel during the reaction to prevent critical oxidation. When the solution was preheated to 80 °C, ammonium hydroxide (20 mL) was added to achieve alkaline conditions. After 30 min, black superparamagnetic MNPs were obtained by sedimentation with the help of an external permanent magnet and the supernatant was decanted. The MNPs were washed with deionized water several times (150 mL each time) to remove unreacted chemicals until a stable ferrofluid was obtained.

Superparamagnetic silica nanoparticles: The superparamagnetic MNPs were coated with silica by using a sol-gel method. Superparamagnetic MNPs (0.120 g) was redispersed in 2-propanol (240 mL) and deionized water (18 mL) by sonication for approximately 15 min. Then, under continuous mechanical stirring (800 rpm), ammonium hydroxide (21 mL) and TEOS (4 mL) were consecutively added to the reaction mixture. The reaction proceeded at room temperature for 14 h under continuous mechanical stirring. The resultant product was obtained by magnetic separation with the help of an external permanent magnet and was thoroughly washed with deionized water.

MIP or NMIP: For the preparation of BHb-imprinted polymer, BHb (0.01 g) was dissolved in sodium phosphate buffer (5 mL, pH 7.2) containing APBA (100 mM), and the mixture was incubated at room temperature for 1 h. After adding silica-coated MNPs (0.04 g), the solution was then incubated for 2 h at room temperature. Prior to use, the silica-coated MNPs were subjected to extensive deionized water, and washed thoroughly. Subsequently, a 100 mM aqueous solution of ammonium persulfate (6.5 mL) as initiator was slowly added dropwise to the above solution for about 20 min and the polymerization process was executed at room temperature. After 14 h, BHb imprinted polymer were obtained. Finally, the template-containing MIP-coated MNPs were washed with 0.2 M sodium phosphate buffer (pH 9.0) containing 0.5 M sorbitol to remove the entrapped template molecules. The MIP-coated MNPs were then equilibrated with the buffer used in the polymerization process.

NMIP was prepared using the same procedure but without BHb.

Characterization

The crystal structure of the nanoparticles was determined by XRD. The XRD pattern of each sample was recorded with a Shimadzu (Japan) D/Max-2500 diffractometer, using a monochromatized X-ray beam with nickel-filtered $Cu_{K\alpha}$ radiation. The XRD patterns were collected in the range of $5° < 2\theta < 80°$ with a dwelling time of 2 s and a scan rate of 6.0°/min. The substance was automatically searched using the JCPDS-International Center for Diffraction Data.

The size and morphology of the nanoparticles were measured by a FEI (Netherlands) Tecnai-20 TEM instrument. The nanoparticle sample dispersed in hexane solution was cast onto a carbon-coated copper grid sample holder followed by evaporation at room temperature.

TGA was performed for powder samples (~10 mg) with a heating rate of $10\,°C \cdot min^{-1}$ using a Netzsch STA 409 (Germany) thermogravimetric analyzer under a nitrogen atmosphere up to 1000 °C.

Magnetic properties were measured with a LDJ9600–1 (United States) VSM at room temperature.

Protein Adsorption Experiments

Rebinding conditions remained similar to the synthetic conditions. The amount of protein adsorbed onto the MIP-coated MNPs was calculated from the differences in the protein concentrations before and after incubation on the rotator (100 rpm). The protein concentrations were measured with a Shimadzu (Japan) UV-2450 spectrophotometer at 405 nm for BHb. The eluting solution was prepared by mixing a 0.5 M aqueous solution of sorbitol (80 mL) and 0.2 M sodium phosphate buffer (pH 9.0, 20 mL). Before elution, the nanoparticles were washed thoroughly with deionized water to remove the non-adsorbed protein.

The experimental data are presented as the adsorption capacity per unit mass (mg) of the nanoparticles, and the adsorption capacity (Q) is calculated using Eq. (6):

$$Q = (C_0 - C_s) \times V\,m^{-1} \quad (6)$$

Here C_0 ($mg\,mL^{-1}$) is the initial concentration of protein solution, C_s ($mg\,mL^{-1}$) is the protein concentration of the supernatant, V (mL) is the volume of the initial solution and m (mg) is the mass of the nanoparticles.

Acknowledgements

The authors are grateful to National Basic Research Program (973 Program No.2007CB914100, 863 Program No.2007AA10Z432), the National Natural Science Foundation of China (No.20675040, 20875050) and the Natural Science Foundation of Tianjin (No.07JCYBJC00500) for financial support.

[1] A. K. Gupta, M. Gupta, *Biomaterials* **2005**, *26*, 3995–4021.
[2] S. Bucak, D. A. Jones, P. E. Laibinis, T. A. Hatton, *Biotechnol. Prog.* **2003**, *19*, 477–484.
[3] K. S. Lee, I. S. Lee, *Chem. Commun.* **2008**, 709–711.
[4] S. M. O'Brien, O. R. T. Thomas, P. Dunnill, *J. Biotechnol.* **1996**, *50*, 13–25.
[5] G. Wulff, *Angew. Chem.* **1995**, *107*, 1958–1979, *Angew. Chem. Int. Ed. Engl.* **1995**, *34*, 1812–1832.
[6] M. Yan, O. Ramström, *CRC Press* **2005**.
[7] L. Ye, K. Mosbach, *Chem. Mater.* **2008**, *20*, 959–868.
[8] E. Turiel, A. Martin-Esteban, *Anal. Bioanal. Chem.* **2004**, *378*, 1876–1886.
[9] H. Zhang, L. Ye, K. Mosbach, *J. Mol. Recognit.* **2006**, *19*, 248–259.
[10] G. Wulff, *Chem. Rev.* **2002**, *102*, 1–28.
[11] K. Haupt, K. Mosbach, *Chem. Rev.* **2000**, *100*, 2495–2504.
[12] C. Alvarez-Lorenzo, A. Concheiro, *J. Chromatogr. B* **2004**, *804*, 231–245.
[13] N. W. Turner, C. W. Jeans, K. R. Brain, C. J. Allender, V. H. Hlady, D. W. Britt, *Biotechnol. Prog.* **2006**, *22*, 1474–1489.
[14] X. Zhou, W. Y. Li, X. W. He, L. X. Chen, Y. K. Zhang, *Sep. Purif. Rev.* **2007**, *36*, 257–283.
[15] N. W. Turner, X. Liu, S. A. Piletsky, V. Hlady, D. W. Britt, *Biomacromolecules* **2007**, *8*, 2781–2787.
[16] M. Kempe, M. Glad, K. Mosbach, *J. Mol. Recognit.* **1995**, *8*, 35–39.
[17] H. Q. Shi, W. B. Tsai, M. D. Garrison, S. Ferrari, B. D. Ratner, *Nature* **1999**, *398*, 593–597.
[18] C. L. Yan, Y. Lu, S. Y. Gao, *J. Polym. Sci. Part A* **2007**, *45*, 1911–1919.
[19] A. Bossi, S. A. Piletsky, E. V. Piletska, P. G. Righetti, A. P. F. Turner, *Anal. Chem.* **2001**, *73*, 5281–5286.
[20] P. C. Chou, J. Rick, T. C. Chou, *Anal. Chim. Acta* **2005**, *542*, 20–25.
[21] F. Bonini, S. Piletsky, A. P. F. Turner, A. Speghini, A. Bossi, *Biosens. Bioelectron.* **2007**, *22*, 2322–2328.
[22] T. Shiomi, M. Matsui, F. Mizukami, K. Sakaguchi, *Biomaterials* **2005**, *26*, 5564–5571.
[23] C. J. Tan, H. G. Chua, K. H. Ker, Y. W. Tong, *Anal. Chem.* **2008**, *80*, 683–692.

[24] R. J. Ansell, K. Mosbach, *Analyst* **1998**, *123*, 1611–1616.
[25] M. Yamaura, R. L. Camilo, L. C. Sampaio, M. A. Macêdo, M. Nakamura, H. E. Toma, *J. Magn. Magn. Mater.* **2004**, *279*, 210–217.
[26] S. Mornet, F. Grasset, J. Portier, E. Duguet, *Eur. Cells Mater.* **2002**, *3*, 110–113.
[27] X. Q. Liu, Z. Y. Ma, J. M. Xing, H. Z. Liu, *J. Magn. Magn. Mater.* **2004**, *270*, 1–6.
[28] C. Y. Wang, G. M. Zhu, Z. Y. Chen, Z. G. Lin, *Mater. Res. Bull.* **2002**, *37*, 2525–2529.
[29] L. Ye, P. A. G. Cormack, K. Mosbach, *Anal. Commun.* **1999**, *36*, 35–38.
[30] G. Yin, Z. Liu, J. Zhan, F. X. Ding, N. J. Yuan, *Chem. Eng. J.* **2002**, *87*, 181–186.

Received: August 4, 2008
Published online: November 28, 2008

